2024 IEEE 14th International Conference
"Nanomaterials: Applications & Properties" (IEEE NAP-2024)
Riga, Latvia, Sep. 8-13, 2024

Non-Equivalence of Interatomic Interaction in Model Calculations of the Phonon Dispersion

Ivan Nebola
Uzhhorod National University
Uzhhorod, Ukraine
ivan.nebola@uzhnu.edu.ua

Diana Kaynts
Uzhhorod National University
Uzhhorod, Ukraine
diana.kaynts@uzhnu.edu.ua

Olga Maksakova
Kharkiv National University
Kharkiv, Ukraine
maksakova.tereshenko@gmail.com

Anton Katanytsia
Uzhhorod National University
Uzhhorod, Ukraine
katanitsyaanton@gmail.com

Ihor Shkirta
Mukachevo State University
Mukachevo, Ukraine
imshkirta@gmail.com

Andrii Korneichuk
Uzhhorod Nationa University
Uzhhorod, Ukraine
andrii.korneichuk@uzhnu.edu.ua

2024 IEEE 14th International Conference Nanomaterials: Applications & Properties (NAP) | 979-8-3503-8012-5/24/$31.00 ©2024 IEEE | DOI: 10.1109/NAP62956.2024.10739699

***Abstract*— Consecutive inclusion of additional physical parameters (color, phase, sign of charge, spin, etc.) in the symmetric description led to creation of the theory of color symmetry and the concept of superspatial symmetry. Being based on the latter approach, a method for calculating the phonon dependences of complex crystals was developed in continuation. Among the varieties of generalized symmetry, the concept of superspatial symmetry is quite convenient and visual when constructing (3+d) dimensional models for describing the crystal structure of complex crystals and systems united by a single metric and scale of the protocrystal carrier function. Software was developed and model calculations of phonon spectra of crystals of $BaTiO_3$ type crystals in equidistant and non-equidistant approximations for the field of force interaction were carried out. It is shown that the non-physical 5-fold degeneracy at the point R of the Brillouin zone in the calculations in the equidistant approximation of the force field splits when considering the non-equivalent force interaction.**

Keywords—phonon, dispersion, super speisymmetry, power constant, crystal structure

I. Introduction

The concept of superspace symmetry was initiated in the papers of de Wolff and his colleagues [1] in the 80s of the last century, was developed in various mathematical directions and physical applications. Its main direction can be considered its application for reviewing of problems of generalized symmetry Its main direction can be considered its application for reviewing of problems of generalized symmetry [2] and description of the crystal structure of incommensurable phases and comparison of its methods with traditional approaches [3,4]. A number of physical applications were also developed [5,6]. In continuation of the paper [7], a method was developed for calculating model phonon spectra of complex crystals of cubic syngonia in the equidistant approximation [8,9].Formation of the (3+d) dimensional metric of the protocrystal is based on its higher symmetry and is associated with an additional d-dimensional space [7], which allows the description of real objects (crystals and systems) as natural (sa×sa×sa)-superlattices [8,9]. The use of a complete set of modulation vectors makes it possible to determine the amplitudes of the mass modulation functions and the Fourier components of the dynamic matrices. Being based on them, it is possible to generate a generalized dynamic matrix, in the form of a superposition of the Fourier components of the dynamic matrices of the protocrystal, built based on different starting points localized in occupied positions of the protocrystal, and determined taking into account their composition at various points of the Brillouin zone, connected by modulation vectors, and mass perturbation matrices described by amplitudes of mass modulation functions.

The compositional features of the realization of complex crystals and systems by the mechanism of filling with atoms of different types and vacancies, translationally equivalent positions given by the basis of the protocrystal, are covered by the concept of superspatial symmetry [4]. Dispersion curves of the phonon spectrum of complex crystals are defined as solutions of the matrix equation:

$$|A - \omega^2 B| = 0, \qquad (1)$$

where A is formed from the Fourier components of the dynamic matrices of a monatomic protocrystal. Matrix B is formed in a similar way from the amplitudes of mass modulation functions [2-4]. Dynamic matrices of a monatomic protocrystal $D_{\alpha\beta}(k + q_i)$ are determined from the relation [4-5]

$$D_{\beta\gamma}(k + q_i) = \sum_{(l \neq 0)} \alpha_n \frac{l_\beta l_\gamma}{l^2} \left(1 - e^{i(k+q_i)l}\right) \qquad (2)$$

where α_n – the force constant of the interaction between the atom in the 0-th position and the atom in the l-th position, l_β, l_γ are the projections of the l vector on the β, γ axis.

II. Calculations

One of the simplest families of crystal structures that can be described as (sa×sa×sa) superlattices, namely, as (2a×2a×2a) superlattice based on a simple cubic lattice (SCL) (Fig. 1) is a family of the perovskite class. We will use it as an illustration of the calculation method.

At the same time, we note the difference in the combinations of filling the orbits with atoms depending on the choice of localization of the starting point for describing the motif of the structure (Fig. 2) (a well-known setting for describing the perovskite motif).

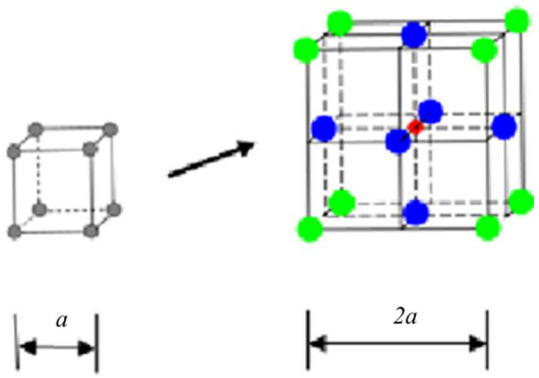

Fig. 1. The structure of the $BaTiO_3$ crystal as a (2a×2a×2a) superlattice based on SCL.

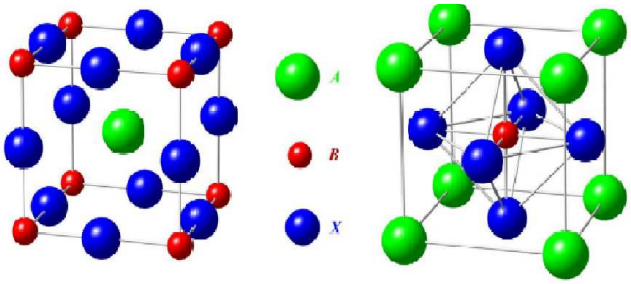

Fig. 2. Crystal structure of the ABX_3 type of an ideal cubic perovskite with different starting points for describing the motif: the starting point is related to the Ti (a) and Ba (b) atoms.

Thus, the composite superlattice is obtained modulating SCL by using 8 modulation vectors for the (2a×2a×2a)-superlattice. The implementation of description of real crystal structures by choosing (3+d)-dimensional bases [7-9] allows us to introduce a description that covers the possibility of filling the SCL positions of the structures with (sa×sa×sa)-superlattices. This description of crystal formations of cubic syngonia with (sa×sa×sa)-superlattices is embedded in (3+d)-dimensional bases:

direct:
a_1 = (a, 0, 0, −b/s, 0, 0);
a_2 = (0, a, 0, 0, −b/s, 0);
a_3 = (0, 0, a, 0, 0, −b/s);
a_4 = (0, 0, 0, b, 0, 0);
a_5 = (0, 0, 0, 0, b, 0);
a_6 = (0, 0, 0, 0, 0, b)

and inverse:
a_1^* = (2π/a, 0, 0, 0, 0, 0);
a_2^* = (0, 2π/a, 0, 0, 0, 0);
a_3^* = (0, 0, 2π/a, 0, 0, 0);
a_4^* = (2π/sa, 0, 0, 2π/b, 0, 0);
a_5^* = (0, 2π/sa, 0, 0, 2π/b, 0);
a_6^* = (0, 0, 2π/sa, 0, 0, 2π/b).

The (3+d)-dimensional description of $BaTiO_3$ crystals with a (2a×2a×2a)-superlattice covers a set of eight modulation vectors, which can be decomposed into 4 stars:

1. (0, 0, 0) – dimensionality one;
2. (π/a, π/a, 0) – dimensionality three;
3. (π/a, π/a, π/a) – dimensionality one;
4. (π/a, 0, 0) – dimensionality three.

The motif of the structure allows us to determine eight possible initial starting points for formation of the orbit, which are given by the radius vectors: r_{Ti} = (0, 0, 0), r_O = (2a(1/2, 0, 0), 2a(0, 1/2, 0), 2a(0, 0, 1/2)) r_{Ba} = 2a(1/2, 1/2, 1/2), r_{Vac} = (2a(1/2, 1/2, 0), 2a(1/2, 0, 1/2), 2a(0. 1/2, 1/2). Fig. 2a shows the setup with the starting point localized on the Ti atom.

Note that the implementation of any motif of a real crystal is carried out by filling specific positions of the superlattice. The solution of the system of equations (3) allows us to determine the mass distribution function given in the form of a superposition of the modulation functions $\rho_j = \rho(q_j, b_j^*)$:

$$m(r_k, \tau_k) = \sum_{j=0}^{8} \rho\,(q_j, b_j^*) exp\{i(q_j r_k + b_j^* \tau_l)\} \quad (3)$$

Solutions (3) (for any fixed value of τ) of crystals (ABC_3D_3) take the form

$$\begin{aligned}
\rho(q_1) &= \frac{m_1+m_2+m_3+m_4+m_5+m_6+m_7+m_8}{8};\\
\rho(q_2) &= \frac{m_1-m_2+m_3+m_4-m_5-m_6+m_7-m_8}{8};\\
\rho(q_3) &= \frac{m_1+m_2-m_3+m_4-m_5+m_6-m_7-m_8}{8};\\
\rho(q_4) &= \frac{m_1+m_2+m_3-m_4+m_5-m_6-m_7-m_8}{8};\\
\rho(q_5) &= \frac{m_1-m_2-m_3+m_4+m_5-m_6-m_7+m_8}{8};\\
\rho(q_6) &= \frac{m_1-m_2+m_3-m_4-m_5+m_6-m_7+m_8}{8};\\
\rho(q_7) &= \frac{m_1+m_2-m_3-m_4-m_5-m_6+m_7+m_8}{8};\\
\rho(q_8) &= \frac{m_1-m_2-m_3-m_4+m_5+m_6+m_7-m_8}{8}.
\end{aligned} \quad (4)$$

Here m_j is the mass at position i, $\rho(q_i)$= ρ_i – amplitudes of the mass modulation functions

After introducing the motif of $BaTiO_3$ crystals, the solutions of the system of equations (4) take the form:

$$\begin{aligned}
\rho_0 &= \frac{m_A+m_B+3m_C+m_D}{8}\\
\rho_1 &= \frac{m_A-m_B-3m_C+3m_D}{8}\\
\rho_2 &= \frac{m_A+m_B-m_C-m_D}{8}\\
\rho_3 &= \frac{m_A-m_B+m_C-m_D}{8}
\end{aligned} \quad (5)$$

The determined values of the amplitudes of the mass modulation functions allow forming the mass defect matrix B in the form

$$B = \rho(q_i - q_j) = \begin{pmatrix} \rho_1 & \rho_2 & \rho_3 & \rho_4 & \rho_5 & \rho_6 & \rho_7 & \rho_8 \\ \rho_2 & \rho_1 & \rho_5 & \rho_6 & \rho_3 & \rho_4 & \rho_8 & \rho_7 \\ \rho_3 & \rho_5 & \rho_1 & \rho_7 & \rho_2 & \rho_8 & \rho_4 & \rho_4 \\ \rho_4 & \rho_6 & \rho_7 & \rho_1 & \rho_8 & \rho_2 & \rho_3 & \rho_5 \\ \rho_5 & \rho_3 & \rho_2 & \rho_8 & \rho_1 & \rho_7 & \rho_6 & \rho_4 \\ \rho_6 & \rho_4 & \rho_8 & \rho_2 & \rho_7 & \rho_1 & \rho_5 & \rho_3 \\ \rho_7 & \rho_8 & \rho_4 & \rho_3 & \rho_6 & \rho_5 & \rho_1 & \rho_2 \\ \rho_8 & \rho_7 & \rho_6 & \rho_5 & \rho_4 & \rho_3 & \rho_2 & \rho_1 \end{pmatrix} \otimes \begin{pmatrix} 1 & 0 & 0 \\ 0 & 1 & 0 \\ 0 & 0 & 1 \end{pmatrix} \qquad (6)$$

Formation of the generalized dynamic matrix A is related with determination of the Fourier components of the dynamic matrices of a monoatomic protocrystal. To do this, we modify the relation (2), assuming a dependence on the type of interacting atoms for the force constant:

$$D^p_{\beta\gamma}(k + q_i) = \sum_{(l \neq 0)} \alpha^p_l \frac{l_\beta l_\gamma}{l^2}\left(1 - e^{i(k+q_i)l}\right) \qquad (7)$$

where the index p specifies the localization of the starting point. Let us set for the dynamic matrices $D_{\beta\gamma}(k + q_i)$ a system similar to (3) and determine $\rho\left(D^p_{\beta\gamma}(k + q_i), (q_i - q_j)\right)$ and write the matrix A in the form

$$\mathrm{A} = \rho\left(D^p_{\beta\gamma}(k + q_i), (q_i - q_j)\right) = \rho\left(D_{(q_i - q_j)}(k + q_j)\right) = D_{(q_i - q_j)}(k, q_j)$$

$$= \begin{pmatrix} D_{q_1}(k,q_1) & D_{q_2}(k,q_1) & D_{q_3}(k,q_1) & D_{q_4}(k,q_1) & D_{q_5}(k,q_1) & D_{q_6}(k,q_1) & D_{q_7}(k,q_1) & D_{q_8}(k,q_1) \\ D_{q_2}(k,q_2) & D_{q_1}(k,q_2) & D_{q_5}(k,q_2) & D_{q_6}(k,q_2) & D_{q_3}(k,q_2) & D_{q_4}(k,q_2) & D_{q_8}(k,q_2) & D_{q_7}(k,q_2) \\ D_{q_3}(k,q_3) & D_{q_5}(k,q_3) & D_{q_1}(k,q_3) & D_{q_7}(k,q_3) & D_{q_2}(k,q_3) & D_{q_8}(k,q_3) & D_{q_4}(k,q_3) & D_{q_6}(k,q_3) \\ D_{q_4}(k,q_4) & D_{q_6}(k,q_4) & D_{q_7}(k,q_4) & D_{q_1}(k,q_4) & D_{q_8}(k,q_4) & D_{q_2}(k,q_4) & D_{q_3}(k,q_4) & D_{q_5}(k,q_4) \\ D_{q_5}(k,q_5) & D_{q_3}(k,q_5) & D_{q_2}(k,q_5) & D_{q_8}(k,q_5) & D_{q_1}(k,q_5) & D_{q_7}(k,q_5) & D_{q_6}(k,q_5) & D_{q_4}(k,q_5) \\ D_{q_6}(k,q_6) & D_{q_4}(k,q_6) & D_{q_8}(k,q_6) & D_{q_2}(k,q_6) & D_{q_7}(k,q_6) & D_{q_1}(k,q_6) & D_{q_5}(k,q_6) & D_{q_3}(k,q_6) \\ D_{q_7}(k,q_7) & D_{q_8}(k,q_7) & D_{q_4}(k,q_7) & D_{q_3}(k,q_7) & D_{q_6}(k,q_7) & D_{q_3}(k,q_7) & D_{q_1}(k,q_7) & D_{q_2}(k,q_7) \\ D_{q_8}(k,q_8) & D_{q_7}(k,q_8) & D_{q_6}(k,q_8) & D_{q_5}(k,q_8) & D_{q_4}(k,q_8) & D_{q_3}(k,q_8) & D_{q_2}(k,q_1) & D_{q_1}(k,q_8) \end{pmatrix}_1$$

To record the matrix A, compact abbreviations for the notation $\rho\left(D^p_{\beta\gamma}(k + q_i), (q_i - q_j)\right)$ were used.

Note that the transition from a non-equidistant approximation to a non-equidistant approximation is due to the use of relations (2) and (7) in the formation of matrix A. In particular, the use of relation (2) brings the matrix to a dianonal form.

To solve the system, software was developed and model calculations of phonon dispersion [10] in equidistant (Fig. 3) and non-equidistant (Fig. 4) approximations for the force field were carried out [9].

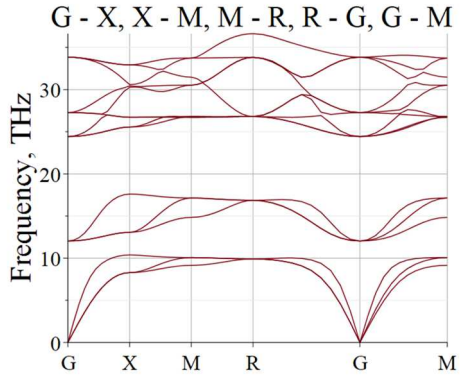

Fig. 3. Phonon spectra of the $BaTiO_3$ crystal in the equidistant approximation.

Analysis of the calculations showed that no complication of the force field within the equidistant approximation ensures the presence of a non-physical five-fold degeneracy and the point R (to demonstrate a wide set of force constants including non-physical interactions between atoms and vacancies is presented (Table 1)) . At the same time, the non-equivalent approximation for the force field removes the unphysical degeneracy at the point R when type-dependent force constants are introduced at the distances [1,1,0], [2,0,0], etc.

TABLE I. FORCE CONSTANTS A_N (N/M) [X-VACANCY]

1 | Distance [1,0,0]:	[[[Ti, O], 220], [[Ba, X], 220], [[Ti, X], 220], [[O, X], 220], [[X, X], 220]]
2 | Distance [1,1,0]:	[[[Ba, O], 110], [[O, O], 110], [[Ba, X], 110], [[Ti, X], 110], [[O, X], 110], [[X, X], 110]]
3 | Distance [1,1,1]:	[[[Ba, Ti], 10], [[Ba, X], 10], [[Ti, X], 10], [[O, X], 10], [[X, X], 10]]
4 | Distance [2,0,0]:	[[[Ba, Ba], 5], [[Ti, Ti], 5], [[O, O], 5], [[Ba, X], 5], [[Ti, X], 5], [[O, X], 5], [[X, X], 5]]
5 | Distance [2,1,0]:	[[[Ti, O], 3.5], [[Ba, X], 3.5], [[Ti, X], 3.5], [[O, X], 3.5], [[X, X], 3.5]]
6 | Distance [2,1,1]:	[[[Ba, O], 2], [[O, O], 2], [[Ba, X], 2], [[Ti, X], 2], [[O, X], 2], [[X, X], 2]]
7 | Distance [2,2,0]:	[[[Ba, Ba], 1], [[Ti, Ti], 1], [[O, O], 1], [[Ba, X], 1], [[Ti, X], 1], [[O, X], 1], [[X, X], 1]]
8 | Distance [2,2,1]:	[[[Ti, O], 0.5], [[Ba, X], 0.5], [[Ti, X], 0.5], [[O, X], 0.5], [[X, X], 0.5]]
9 | Distance [2,2,2]:	[[[Ti, O], 0.25], [[Ba, X], 0.25], [[Ti, X], 0.25], [[O, X], 0.25], [[X, X], 0.25]]

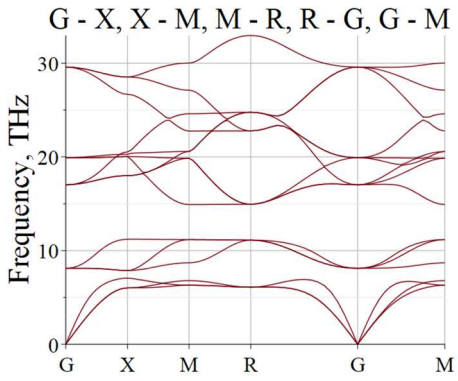

Fig. 4. Phonon spectra of the $BaTiO_3$ crystal in the equidistant approximation.

TABLE II. FORCE CONSTANTS AN (N/M) [X-VACANCY]

1 | Distance [1,0,0]:	[Ti, O], 220
2 | Distance [1,1,0]:	[[Ba, O], 105], [[O, O], 115]],
3 | Distance [1,1,1]:	[Ba, Ti], 10],
4 | Distance [2,0,0]:	[[Ba, Ba], 7], [[Ti, Ti], 6], [[O, O], 5]],
5 | Distance [2,1,0]:	[Ti, O], 3.5],
6 | Distance [2,1,1]:	[[Ba, O], 2], [[O, O], 1],
7 | Distance [2,2,0]:	[[Ba, Ba], 1], [[Ti, Ti], 0.7], [[O, O], 0.5]]
8 | Distance [2,2,1]:	[Ti, O], 0.25],
9 | Distance [2,2,2]:	[[Ti, O], 0.125]],

III. CONCLUSIONS

It is shown that depending on the choice of the equidistant approximation [3,4] (the force constants are determined only by the distance between the positions of different orbits and do not depend on the type of interacting atoms) and the non-equidistant approximation for the force constants α_n (the force constants also depend on the type of interacting atoms) the calculated model phonon spectra of $BaTiO_3$ crystals satisfactorily describe the values of the experimental data in the center of the Brillouin zone (G(Γ)). At the same time, calculations in the equidistant approximation lead to a nonphysical five-fold degeneracy at the point R (the value near 25 THz), which is removed at transition to non-equivalent approximation.

REFERENCES

[1] P. M. De Wolff, T. Janssen, A. Janner, “The superspace groups for incommensurate crystal structures with a one-dimensional modulation,” Acta Cryst. A, vol. 37,pp. 625–636, 1981.

[2] J. M. Pérez-Mato, G. Madariaga, and M. J. Tello, “Superspace groups and Landau theory. A physical approach to superspace symmetry in incommensurate structures,” Phys. Rev. B, vol. 30, pp. 1534–1543, 1984.

[3] Sander van Smaalen, Branton J Campbell, Harold T Stokes, “Equivalence of superspace groups,” A Multinational Journal, vol. 16, ID 41, 1989.

[4] Massimo Nespolo, Mois Ilia Aroyo and Bernd Souvignier, “Crystallographic shelves: space-group hierarchy explained,” Journal of Applied Crystallography, vol. 51, no. 5, pp. 1481–1491, 2018.

[5] Ivan Orlov, Lukas Palatinus and Gervais Chapuis, J. Appl. Cryst., vol. 41, pp. 1182–1186, 2008.

[6] M. Perez-Mato, J.I. Ribeiro, V. Petricek and M.I. Aroyo, “Magnetic superspace groups and symmetry constraints in incommesurate magnetic phases,” J. Phys.: Condens Matter, vol. 24, pp. 163201–163221, 2012.

[7] T. Janssen, “On the lattice dynamics of incommensurate crystal phases,” J. Phys. C: Solid State Phys, vol. 12, no. 24, pp. 5381–5392, 1979.

[8] I.I. Nebola, A.Ya. Shteyfan, V.I. Sidey, A.F. Katanytsia, I.P. Studenyak, I.M. Shkyrta, “Model research of phonon spectra of argyrodites family,” Semiconductor Physics, Quantum Electronics & Optoelectronics, vol. 21, no. 2, pp. 134–138, 2018.

[9] I.I. Nebola, A.F. Katanytsia, A.Ya. Shteyfan, I.M. Shkyrta, I.P. Studenyak, M. Timko, P. Kopčanský, “Model phonon spectra of Cu7SiS5I and Ag7SiS5I crystals,” Semiconductor Physics, Quantum Electronics & Optoelectronics, vol. 23, no. 4, pp. 366–371, 2020.

[10] Software Product (2018) https://maple.cloud/app/5753562177994752/Modeling+of+dispersions+of+ phonon+spectra

МУКАЧІВСЬКИЙ ДЕРЖАВНИЙ УНІВЕРСИТЕТ

89600, м. Мукачево, вул. Ужгородська, 26
тел./факс +380-3131-21109
Веб-сайт університету: www.msu.edu.ua
E-mail: info@msu.edu.ua, pr@mail.msu.edu.ua
Веб-сайт Інституційного репозитарію Наукової бібліотеки МДУ: http://dspace.msu.edu.ua:8080
Веб-сайт Наукової бібліотеки МДУ: http://msu.edu.ua/library/